

## Numerical investigation of the effect of orifice number and diameter in a turbulent jet ignition system on hydrogen combustion

Marcelina Górzynska<sup>1</sup> , Ireneusz Pielecha<sup>1\*</sup> 

<sup>1</sup> Faculty of Civil and Transport Engineering, Poznan University of Technology, ul. J. Rychlewskiego 1, 60-965 Poznan, Poland

\* Corresponding author's e-mail: ireneusz.pielecha@put.poznan.pl

### ABSTRACT

This paper presents the results of a numerical investigation focused on the influence of pre-chamber geometry, specifically, the number and diameter of orifices, on hydrogen combustion characteristics in a turbulent jet ignition (TJI) system. Computational fluid dynamics (CFD) simulations were conducted using AVL FIRE software in two configurations. In the first case, the number of orifices was varied while maintaining a constant diameter, whereas in the second case, the orifice diameter was adjusted to preserve an equivalent total flow cross-sectional area. The obtained results indicate that both geometrical parameters significantly affect the combustion behaviour, particularly in terms of mixture stratification, pressure distribution within the main combustion chamber, and nitrogen oxide (NO) formation. It was determined that the number of orifices exerts a more pronounced effect on combustion performance than their individual diameter. An increased number of orifices with a diameter of 1.5 mm enhanced system efficiency due to improved flow penetration and jet momentum (the most favourable solution is 5 holes with a diameter of 1.5 mm). Under the condition of a constant total discharge area, the configuration comprising 5 orifices with  $d = 1.34$  mm yielded the most favourable results (combustion efficiency was approximately 1% lower than in the best-performing configuration). This configuration ensured stable combustion operation with respect to the analysed performance and emission parameters.

**Keywords:** hydrogen combustion, turbulent jet ignition, pre-chamber, thermodynamic parameters, computational fluid dynamics research.

### INTRODUCTION

#### Turbulent jet ignition system

Current research into combustion technologies primarily focuses on improving engine efficiency, but also aims to reduce harmful emissions into the atmosphere. All of these efforts are driven by environmental regulations and the need for energy transformation. One proposed method is the use of turbulent jet ignition (TJI) technology, which features a pre-chamber [1]. Pre-chambers with independent fuel supply enable the creation of a richer mixture in the combustion chamber, resulting in effective ignition in the main chamber. These processes contribute to improving the

overall combustion kinetics as well as reducing  $\text{NO}_x$  and unburned hydrocarbon emissions [2]. On the basis of the available literature, it can be concluded that the key lies in the research into the design parameters of the pre-chamber and fuel injection conditions, which, together with the geometry of each element, determine the nature of the resulting streams as well as their ability to penetrate through the holes and ignite in the main chamber [3, 4].

A review of the scientific literature on the use of Turbulent Jet Ignition technology indicates that the use of a pre-chamber enables more stable combustion of both lean and ultra-lean fuel mixtures [5, 6]. Experimental and numerical studies using CFD (computational fluid dynamics) techniques

demonstrate that the geometry and design parameters of the pre-chamber, in particular its volume, diameter, and number of holes, shape the nature of the resulting flame jets [7, 8]. This determines the direction and dynamics of combustion front propagation as well as influences the emission of harmful compounds. All additional technologies, such as hydrogen injection into the pre-chamber, also improve process stability and shift the ignition boundary towards very lean mixtures [3, 5]. Selecting appropriate design parameters and ignition conditions for the pre-chamber are key factors determining the further development of TJI technology, fuelled by hydrogen, methane, or ammonia [9, 10].

### **TJI technology in the development of modern combustion engines**

TJI technology is one of the most advantageous lean-burn combustion methods, improving the efficiency of piston engines and reducing harmful emissions. Unlike the classic spark-ignition engine model, TJI technology utilises a pre-chamber where a rich fuel-air mixture ignites. This results in the creation of flame jets that initiate the combustion process, which takes place in the main chamber [8, 11].

TJI technology significantly increases the combustion limit of lean-burn mixtures and significantly reduces  $\text{NO}_x$  emissions by over 90% compared to stoichiometric combustion [8]. This aspect is particularly important in the context of implementing alternative fuels, such as hydrogen, methane, and ammonia, which are difficult to ignite under normal conditions and also have low flame propagation velocity.

### **The influence of the pre-chamber geometry on the combustion process**

The geometry of the pre-chamber – its volume, number and diameter of holes, orientation relative to the main chamber have a decisive influence on the nature and energy of the resulting flame jets. Too many holes weaken the jets, thus weakening their mutual interference, which can result in prolonged combustion time [12, 13]. The studies on the cross-section of holes show that excessively large diameters reduce the pressure difference between the pre-chamber and the main chamber, which directly reduces the possibility of secondary ignition. Changing the nozzle diameter in a natural gas engine directly affects the dynamics of the

resulting flame jets and the combustion stability of ultra-lean mixtures (mixtures with  $\lambda > 2$ ). In comparison, larger holes improve gas exchange, while smaller ones increase the penetration of these jets at the expense of possible flame extinction [11, 13]. The best approach to this problem seems to be the use of small chambers with several holes of 1–2 mm diameter, which allows for rapid and stable ignition while maintaining low emissions [6, 14]. However, in the case of hydrogen, it is also important that the energy from the effluent streams be sufficient to initiate the combustion process at high excess air coefficient values, which in turn requires very precise selection of the number and diameter of holes.

### **Hydrogen combustion in the TJI system**

Although hydrogen is considered one of the most promising fuels, as its use in the engines employing TJI systems is associated with numerous challenges. Combustion efficiency is supported by many factors, including high combustion velocity, a wide ignitability range, and low ignition energy. However, these characteristics can lead to undesirable phenomena, such as pre-ignition or combustion knock. With very lean mixtures, hydrogen requires an intense ignition source, which allows for the initiation of the process occurring throughout the main chamber, and the geometry and volume of the pre-chamber are important for maintaining the stability of the hydrogen combustion process. [13, 14]. In such a case, it is particularly important to precisely determine the effect of the diameter and number of holes in the pre-chamber, which determine both the energy and the ability of flame jets to penetrate the main chamber. The studies on the volume of pre-chambers indicate that the smallest volumes of these chambers, equipped with several relatively large holes, provide the highest indicated efficiency [5]. This is related to reducing heat losses and effectively developing the combustion process in the main chamber [6, 15]. It was also confirmed that the optimal number of holes in the passive chamber was four, and research indicated that a larger number caused jet interference, in addition to significantly slowing down the combustion process. Double-row chambers allowed for more uniform flame spread [5]. The results of these studies confirm that the geometry of both chambers is an important parameter that affects ignition stability and the overall efficiency of the combustion process.

## Injection strategies and the use of alternative fuels in TJI systems

Besides the geometry of the pre-chamber and main chamber, another very important research direction related to the TJI system is the analysis of the use of alternative fuels and the implementation of additional pre-chamber fuelling strategies. Appropriate configuration of the pre-chamber volume and the diameter of the flame outlet holes allows for a high indicated efficiency of approximately 40% and stable hydrogen combustion at a lambda coefficient of 2.6 [13]. To shorten the methanol combustion time, a new swirl accelerating cavity (SAC) chamber concept was developed. Its purpose is to intensify turbulence and accelerate the mixing process and flame propagation within the combustion chamber. This technology shortened methanol combustion time by 28% and shifted the ignition limit to equivalence ratio of 0.35, which in turn contributed to a significant step towards research into the combustion of extremely lean alcohol mixtures [14]. In the case of simulation studies using ammonia with hydrogen addition, it was shown that the high reactivity of the pre-chamber allows for a significant reduction in  $\text{NH}_3$  emissions but leads to an increase in NO emissions. Taking into account the best results, it was indicated here that this is possible using pre-chambers with a larger number of holes with a diameter of approximately 2 mm [10]. Appropriate selection of the timing and dose of fuel injection into the pre-chamber allows for an effective reduction of  $\text{NO}_x$  emissions to approximately 92–99%, thereby increasing the efficiency of the entire system [8]. All conducted studies indicate that further work on the optimisation of the combustion process in the TJI system requires taking into account the geometry of the pre-chamber, the selection of the best parameters and fuel type, and the adjustment of the fuel injection strategy, because the interaction of all these elements affects correct operation of the TJI system.

## Ignition dynamics in the pre-chamber

Studies comparing the ignition timing in the pre-chamber for fuels with different reactivity, including methane and hydrogen, describe differences in flame initiation mechanisms. Hydrogen has a relatively low ignition energy, a high laminar flame burning rate, and a wide flammability limit [9]. These parameters enable the initiation of

combustion of the hydrogen-air mixture in the TJI system with significantly lower energy and shorter exposure time than in the case of methane. The critical Damköhler number, approximately 3.5 times lower than for  $\text{H}_2$  than for  $\text{CH}_4$  (up to approximately 40 vs. approximately 140), is a condition for ignition, which confirms the ease of initiation of hydrogen flame combustion by hot streams formed in the pre-chamber [16]. It has also been shown that there are two different paths in jet ignition: kinetic ignition (jet ignition), which is caused mainly by radicals and the heat generated in the flame jet, and flame ignition, where the flame is transferred to the main chamber [16].

Increasing the pre-chamber nozzle diameter favours the transition from jet to flame ignition.  $\text{H}_2$  ignites at lower Da values and, as it was mentioned earlier, shorter flame jet exposure times in the cylinder, due to, among other things, its significantly higher combustion velocity. A framework for selecting the energy and duration of the jet has been established for ultra-lean mixtures [17]. Numerical studies conducted using DNS show that for the pre-chamber-main chamber system, flame stabilisation on the cylinder side is based primarily on chemical effects (in this case,  $\text{OH}$ ,  $\text{CH}_2\text{O}$ ,  $\text{HO}_2$  radicals) and thermal effects. The combustion velocity in the main chamber can increase to approximately 30x, which is related to the  $\text{CH}_4$  jet being too weak compared to  $\text{H}_2$ , where it is initiated by the same jet enthalpy value. This proves that it is also important to limit the energy emission in the pre-chamber in the case of hydrogen fuel to avoid the possible occurrence of combustion acceleration [17].

## Geometry of the pre-chamber when using hydrogen fuel

When using hydrogen as fuel in a TJI system, the pre-chamber should have a smaller volume, which is directly related to shorter fuel residence time in the chamber and a reduced risk of local pockets containing portions of the rich mixture (typical pre-chamber designs are manufactured from the nickel–chromium alloy Inconel 601). The pre-chamber nozzle should also have a relatively small cross-section to allow for rapid jet formation without choking. The pre-chamber volume and the combined cross-section of the exhaust ports significantly affect the efficiency and timing of ignition in the cylinder. Increasing the volume while maintaining a constant nozzle

size accelerates the ignition initiation in the main chamber. However, one of the most important parameters that limits efficiency is the cross-sectional area of the pre-chamber nozzle. This presents the need to create chambers with a moderate “throat area” for ultra-lean operation [15].

On the other hand, a single-hole diameter that is too small can lead to flame extinction because the jet does not carry the flame front. A diameter that is too large, however, reduces flame velocity and prolongs combustion. In the case of a multi-hole configuration, ignitions are spread across the cylinder volume, shortening the CA10 (thermodynamic start of combustion) and CA90 (end of combustion). The studies conducted with ammonia fuel show that a nozzle that is too narrow can completely prevent ignition in the main chamber [14].

The studies conducted by Wakasugi et al. [18] indicate the use of pre-chambers with orifice diameters ranging from 2.5 to 5 mm. Smaller orifices increase the flame jet velocity, whereas larger ones – around 3.5 mm – lead to a larger flame area. Orifices with a diameter of 5 mm result in the lowest jet velocity, while the flame area lies between those obtained with 2.5 mm and 3.5 mm orifices. According to the research by Frasci et al. [19], increasing the orifice diameter (within the range of 0.5 to 0.9 mm) leads to an increase in the heat release rate, a reduction in specific fuel consumption, and a decrease in the crank angle corresponding to 50% heat release.

The research conducted by Soltic et al. [20] on the evaluation of the efficiency of a TJI engine fuelled with lean methane mixtures indicates that in a four-cylinder gas engine with a pre-chamber, stable combustion conditions were obtained with a global coefficient  $\lambda = 1.7$ . Thermal efficiency above 45% and mean indicated pressure exceeding 20 bar were achieved while maintaining low  $\text{NO}_x$  emissions. The method in which ultra-lean combustion was used resulted in increased unburned methane emissions. The research focusing on the comparison of various pre-chamber geometries showed that increasing the total cross-section of the exhaust nozzles and directing the flame jets deeper into the main chamber enable better flame distribution and more homogeneous combustion of the mixture, while reducing heat losses to the walls. In a subsequent study, a different method was developed for analysing the combustion process between the pre-chamber and the main chamber. This method was based

on simultaneous pressure measurement in both chambers, which allowed for the determination of, i.a. the averaged mass and temperature in the pre-chamber, the total heat released in it, and the enthalpy flux transferred to the cylinder [21]. The effectiveness of this method was confirmed using CFD and data from tests of such an engine, providing information enabling the assessment and further optimisation of the pre-chamber operation.

## PURPOSE AND SCOPE OF RESEARCH WORK

The aim of this research is to demonstrate the greater importance of the number of pre-chamber fuel outlet holes or their diameter. Current studies focus either on the number of orifices [20, 22], their diameter [3, 18, 19, 23], or their angular positioning [24].

Inter-chamber flows in such a combustion system [25, 26] also have a significant influence, affecting both the wall slip phenomenon in various ways [27] and the fuel ignition characteristics inside the pre-chamber [28–30]. In addition to qualitative indicators, it will be important to determine the quantitative relationships between these indicators. The result should be the selection of the best configuration of the number and diameter of the TJI system holes from those proposed in this article. Appropriate pre-chamber geometry (selection of the number and diameter of holes) can improve the efficiency and stability of the combustion process occurring in the TJI system and thus reduce  $\text{NO}_x$  emissions. The results of this research may be particularly important for the engines using fuels such as hydrogen, methane, or ammonia, as in these systems, effective and stable combustion of these lean mixtures poses a challenge for the industry.

## RESEARCH METHODOLOGY

### TJI chamber model

Simulation tests were conducted using AVL Fire 2022.1 software. A movable combustion chamber mesh was used with the parameters presented in Table 1. The mesh represents the combustion chamber of the cylinder with a displacement of  $510.7 \text{ cm}^3$ . The mesh consists of a pre-chamber, a main chamber, and outflow holes.

The mesh is divided into sections representing the elements of the moving mesh. Simulation tests were conducted using a combustion chamber model (without intake and exhaust channels) including four valves and a centrally located pre-chamber. An active pre-chamber system (with fuel feeding) was used. The combustion chamber characteristics are presented in Table 2, and its exemplary view is shown in Figure 1.

A poly-type mesh was used in the study, with a target cell size of 1 mm and a minimum surface cell size of 0.1 mm. Other publications indicate the use of a 3 mm mesh [2, 31], but in the case of a pre-chamber this value appears to be too large. The number of cells in the model is provided in Table 1. The FAME ENGINE PLUS module was used to automate the moving-mesh generation process.

The study accounts for specific initial conditions and several combustion-related models, which are summarised in Table 2.

Figure 1 shows an example view of the TJI combustion chamber model used in numerical studies. The geometry of this model included, among other things, four valves and a centrally located pre-chamber, into which an additional dose of fuel was fed in the active pre-chamber system. The main chamber was devoid of intake and exhaust channels; it was simplified to focus

on the ignition timing and combustion process. The central section shows the system of channels connecting the pre-chamber with the cylinder cavity, through which flame jets pass, initiating combustion of the mixture in the main chamber.

### Input parameters of the model

The research methodology considers a variable number of pre-chamber holes and a variable diameter (assuming a constant flow cross-section). The first test variant involves changing the number of holes while maintaining a constant diameter ( $d = 1.5$  mm). The second variant assumes simultaneous changes in the number and diameter of holes while maintaining a constant flow cross-sectional area. This approach allows for assessing the degree to which the hole distribution itself is more important for flame shape and dynamics, as opposed to their combined cross-section. The proposed combustion chamber variants are presented in Table 3.

The tests were conducted under the following assumptions: a) an active pre-chamber with fuel injection  $q_0_{PC} = 0.4$  mg was used, and a dose of  $q_0_{MC} = 8.3$  mg was injected into the main chamber. Both fuel doses were injected at the same time (injection start  $\alpha = 550$  deg; the fuel injection time is shown in Figure 2).

The tests were conducted in the range of 540 deg (intake valve closing) to 800 deg (exhaust valve opening). Considering charge exchange from the previous engine cycle causes the actual engine cycle to begin at  $\alpha = 360$  deg. Therefore, the so-called hot-TDC occurs at 720 deg. Since the engine has 1.2 bar of boost during intake valve closing, the charge exchange system and its intake were not considered.

**Table 1.** Characteristics of the combustion chamber

|                           |  |
|---------------------------|--|
| Combustion chamber type   | TJI system with pre-chamber and toroidal piston bowl |
| Bore × stroke             | 85 × 90  |
| Compression ratio         | 11.8:1   |
| Number of cells (min/max) | 69,561/234,187                                       |
| Global lambda-value       | 2.5  |

**Table 2.** Initial conditions and models used in the TJI engine simulation

| Initial conditions         |  |
|----------------------------|--|
| Pressure                   | 0.12 MPa   |
| Temperature                | 578 K  |
| Turbulent kinetic energy   | 10 m <sup>2</sup> /s <sup>2</sup>  |
| Turbulent length scale     | 0.003 m  |
| Turbulent dissipation rate | 1732.05 m <sup>2</sup> /s <sup>3</sup>   |
| Models                     |  |
| Combustion                 | Turbulent Flame Speed Closure Model  |
| Spark ignition             | Spark timing = 5 deg bTDC<br>Flame kernel size = 0.003 m<br>Ignition duration 0.0003 s |
| Emission                   | NO model → Extended Zeldovich  |

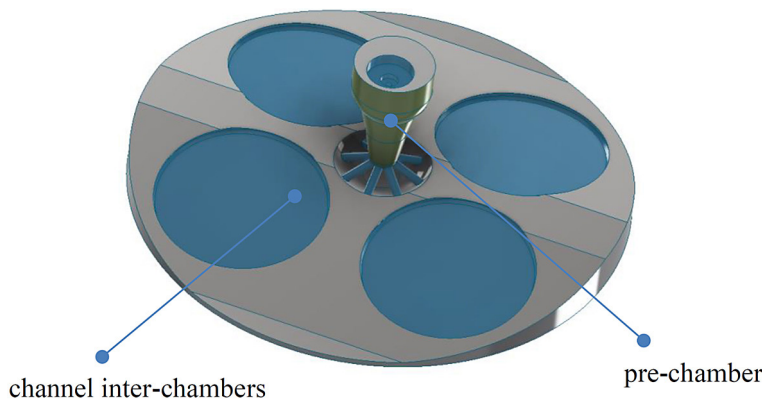
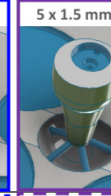
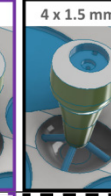
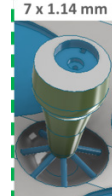
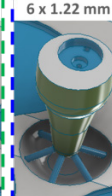
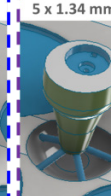
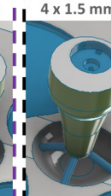


Figure 1. Example view of the TJI system combustion chamber

**Table 3.** Research proposals for the number of holes and diameters of the pre-chamber

| Research variant   | Value  | Visualisation of changes  |  |  |  |
|--|--|---|--|--|--|
| Variable number of orifices: n – without constant total flow area                | $d = 1.5 \text{ mm} = \text{const.}$<br>$n = 4, 5, 6, 7$   |   |   |   |   |
| Variable orifice diameter and number: n, d – constant total flow area maintained | Area = const<br>$n = 4; d = 1.50 \text{ mm}$<br>$n = 5; d = 1.34 \text{ mm}$<br>$n = 6; d = 1.22 \text{ mm}$<br>$n = 7; d = 1.14 \text{ mm}$ |  |  |  |  |

The research presented below is divided into two groups of works: the first one concerns the change in the number of holes (the results of this work are presented in chapter 4 and the change in the number and diameter of holes while maintaining the same value of the flow diameter through the pre-chamber system – chapter 5).

## VARIATION OF ORIFICE NUMBER

### Influence of orifice number variation on charge formation processes

The base value for the hole diameter was assumed to be 1.5 mm. This value is often used in other studies, although they do not always concern hydrogen combustion [32].

The influence of the number of holes has a decisive impact on the quality of charge formation before combustion, i.e., on the preparation of the charge for combustion. In a two-stage combustion system, this is even more important due to

the pre-chamber. Another factor is the additional influence of the passive combustion chamber (without additional injection into the pre-chamber) and active combustion chamber (with additional injection into the pre-chamber). The effect of changing the number of holes on charge formation is shown in Figure 3. This figure shows changes in the spatial charge distribution within a precisely defined angular range – only around the ignition region in PC.

Although the entire combustion chamber is shown in Figure 4, the charge formation in PC is important. In the case of a small number of holes (4), a significant reduction in the  $\lambda$  in PC is visible, which is caused by a large fuel dose in PC (this dose is constant at 0.4 mg – Table 3). This results in a low  $\lambda$ -value and difficulties in ignition of the charge. In the case of 5 holes, the  $\lambda$ -value in the PC is very close to stoichiometric. At  $n = 6$ , a large amount of air is supplied, and the charge is leaner. At  $n = 7$ , a tendency towards stoichiometric charge in the pre-chamber is noted.

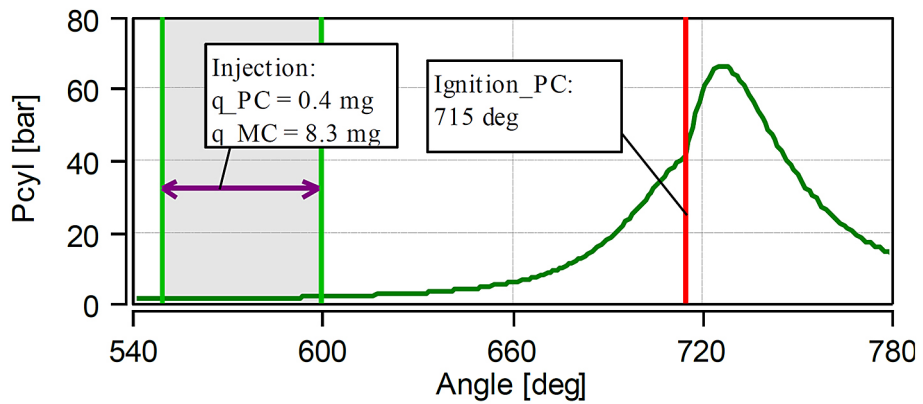


Figure 2. Timing diagram of the injection and ignition of the charge in the TJI system

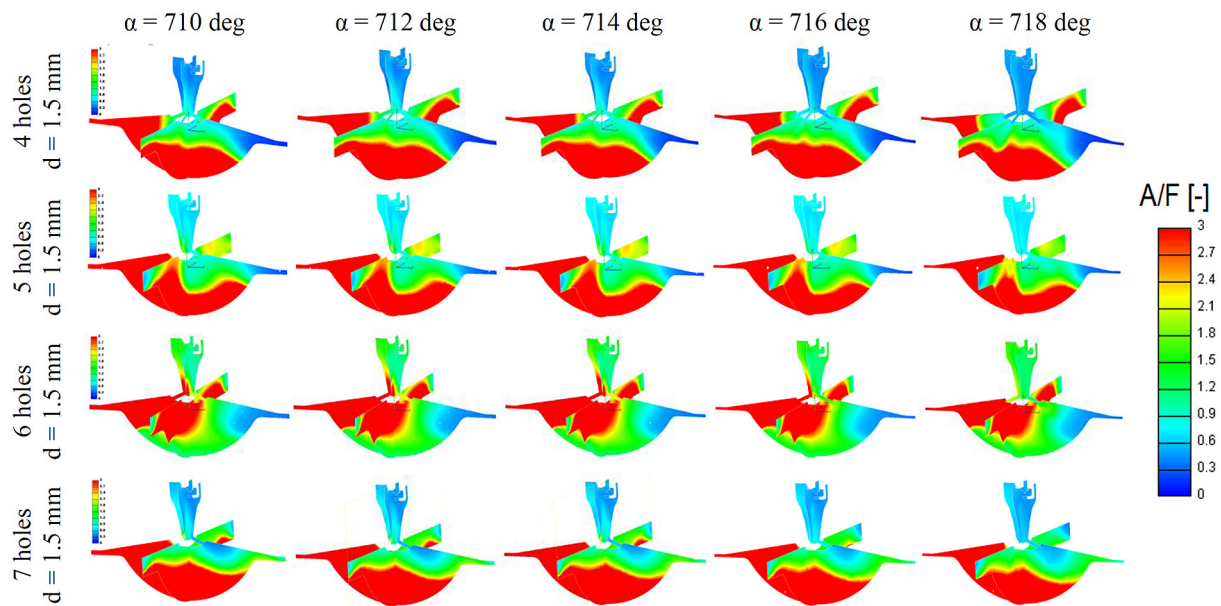


Figure 3. Air-fuel equivalence ratio distribution in a TJI system with a variable number of pre-chamber orifices of constant diameter

This indicates that the number of holes is significant and its relationship to the number of holes is not linear. The analyses above already indicate the presence of stoichiometric charge at  $n = 5$  and 7 holes. This necessitates further thermodynamic analyses to determine the most favourable variant of the pre-chamber geometry in terms of the number of holes.

The next step was to determine the global (rather than local) values of the excess air coefficient. Additionally, the average kinetic energy of turbulence was used to demonstrate its effect on charge formation conditions – Figure 4. Figure 4 shows that the  $\lambda$ -value in PC is not proportional to the number of holes. The large amount of air in PC in Figure 3 is also confirmed in Figure 4, which may result from the highest TKE (turbulent

kinetic energy) value. It is significantly greater (by over 50%) than for the other pre-chamber geometries. As it can be seen from this figure, the global lambda values are similar for  $n = 4, 5$ , and 7 (similar values were also obtained for TKE). The size of the six holes causes the flow through the PC chamber to be slightly different.

Slightly different charge preparation leads to variations in the maximum pressure in the range of 5–6 bar (Figure 5). A large amount of air (at  $n = 6$ ) results in the lowest maximum combustion pressure. Although at  $n = 5$  the  $\lambda$  coefficient in the PC had near-stoichiometric values,  $P_{mx}$  (maximum cylinder pressure) is not the highest here either. The highest  $P_{mx}$  values were obtained at  $n = 7$  ( $P_{mx} = 67.9$  bar); however, the  $P_{mx}$  changes for the remaining curves are small and within 4 bars, which

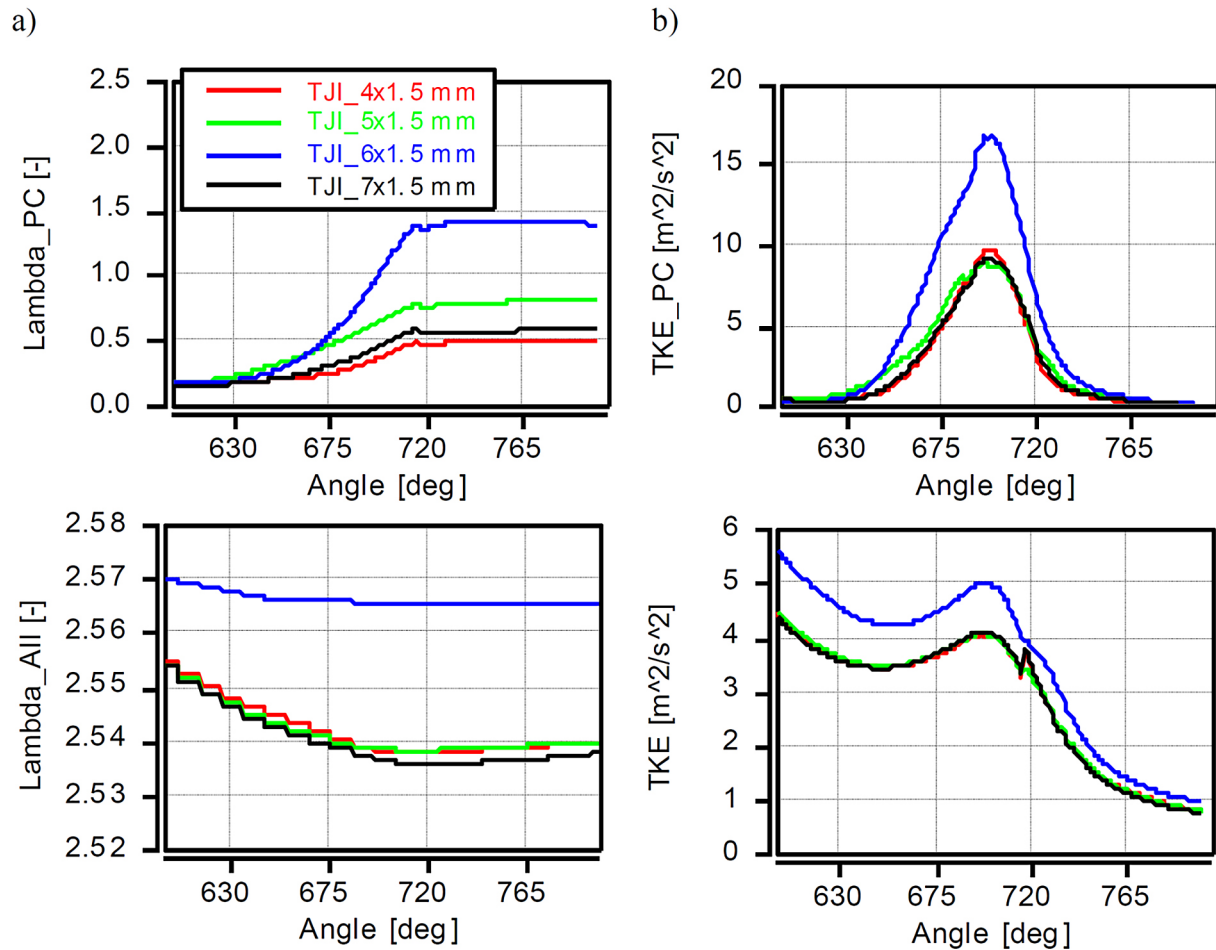


**Figure 4.** Variation of the mean air-fuel equivalence ratio (a) and turbulent kinetic energy (b) in the pre-chamber and main combustion chamber of a TJI system with a variable number of pre-chamber orifices of constant diameter

is a maximum of 7% of the maximum value). However, such small changes can be significant in the analysis of thermodynamic indicators (temperature, heat release rate, heat release and jet velocity from prechamber), as presented in the next chapter.

#### Assessment of thermodynamic conditions

The analysis of thermodynamic processes began with the presentation of local temperature distributions after ignition (which occurred at 716 °CA). Analysis of Figure 6 indicates that the fastest flame development in PC occurs with the smallest and largest number of holes. For  $n = 5$  and  $6$ , flame development in PC is slower, which results from the temperature distribution in PC and its flow to MC. Analysis of this figure indicates the highest possible average temperature value with the smallest number of holes ( $n = 4$  and  $7$ ). The temperature distribution also indicates (regardless of the number of holes) that the

increase in temperature development is consistent with the direction of fuel flow from the pre-chamber. This causes the temperature to reach the piston crown with a considerable delay. However, the engine head is heated very significantly.

Figure 7 shows the effect of the number of holes on the amount and rate of heat release in the pre-chamber and the entire combustion chamber. Such differentiation is only possible during simulations. It is then possible to distinguish between the fuel doses from PC that cause heat release in both chambers independently. Analysing only the conditions in PC does not lead to global conclusions. Although the highest heat amount in the PC was obtained at  $n = 5$  ( $Q_{mx\_PC} = 36.6$  J), the overall analysis does not indicate the best results of this configuration. Here, the best effect was obtained at  $n = 6$  ( $Q_{mx} = 983$  J). Changes in the final  $Q_{mx}$  value in the main chamber reach only 9% of the maximum value. However, the variable number of holes has the greatest impact on the

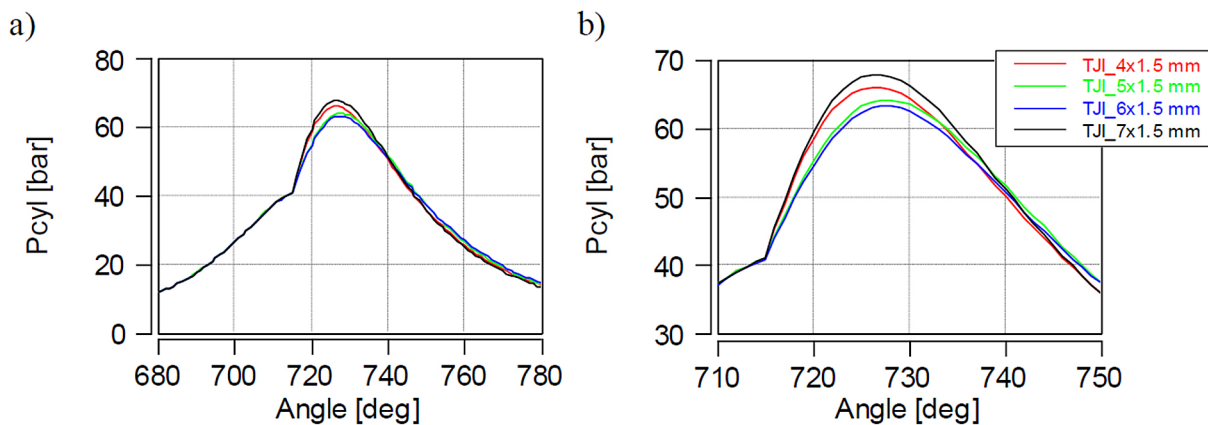


**Figure 5.** Variation of the in-cylinder pressure (a) and its approximation (b) in a Turbulent Jet Ignition (TJI) system with a variable number of constant-diameter pre-chamber orifices

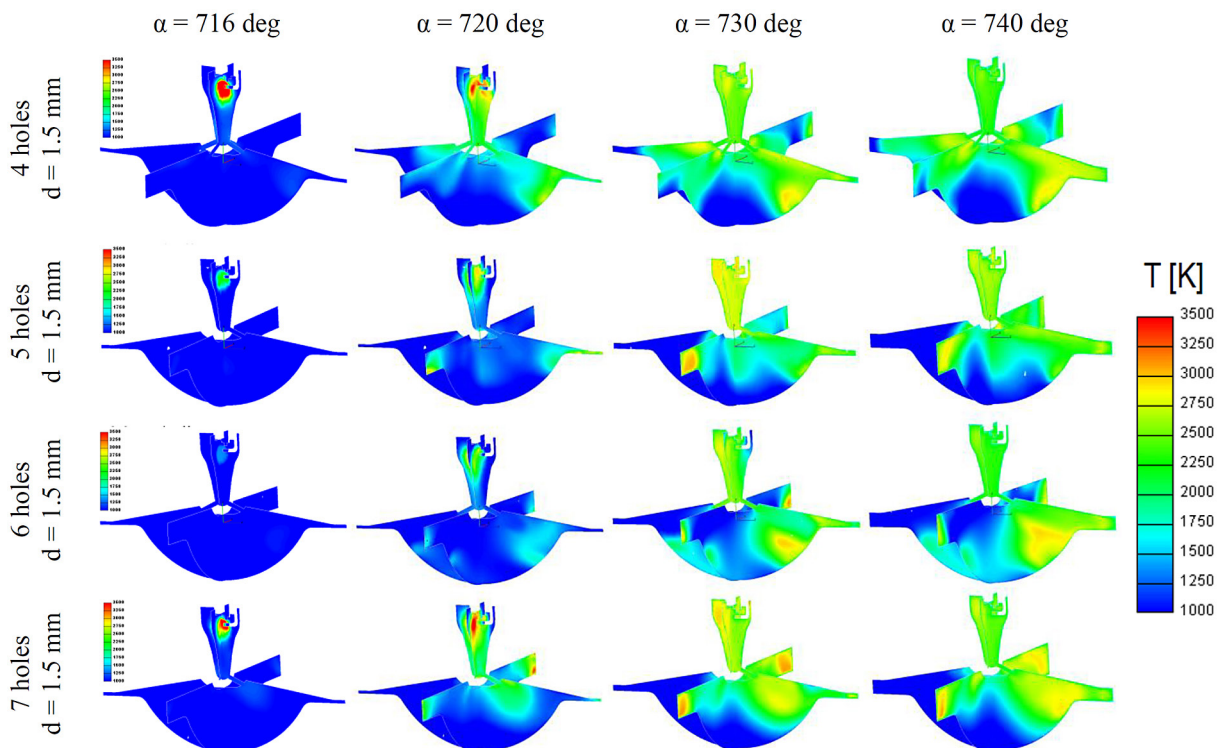


**Figure 6.** Temperature field distribution in a Turbulent Jet Ignition (TJI) system with a variable number of constant-diameter pre-chamber orifices

heat release rate. The maximum rate in PC was obtained at  $n = 7$  ( $dQ_{mx\_PC} = 3.3$  J/deg). Changes amount to a maximum of 20%. Similar conclusions can be drawn by analysing the heat release rate in both spaces. The configuration with  $n = 7$  holes is the best. However, the changes in  $dQ_{mx}$  are much greater. The maximum  $dQ$  value is 56.2 J/deg, but the changes in this value exceed 30% (the lowest values were obtained for  $n = 6$ , with a value of 36.7 J/deg). Similar conclusions can be observed when analysing the average

temperature. The best solution is the  $n = 7$  variant, as the maximum temperature ( $T_{mx} = 1503$  K) occurs early and decreases rapidly. This case also produces the highest combustion pressure (Figure 5), which should result in a high IMEP.

#### Assessment of the discharge velocity of the mixture from the pre-chamber

The previously reported indicators largely account for the rate of outflow of burning flames

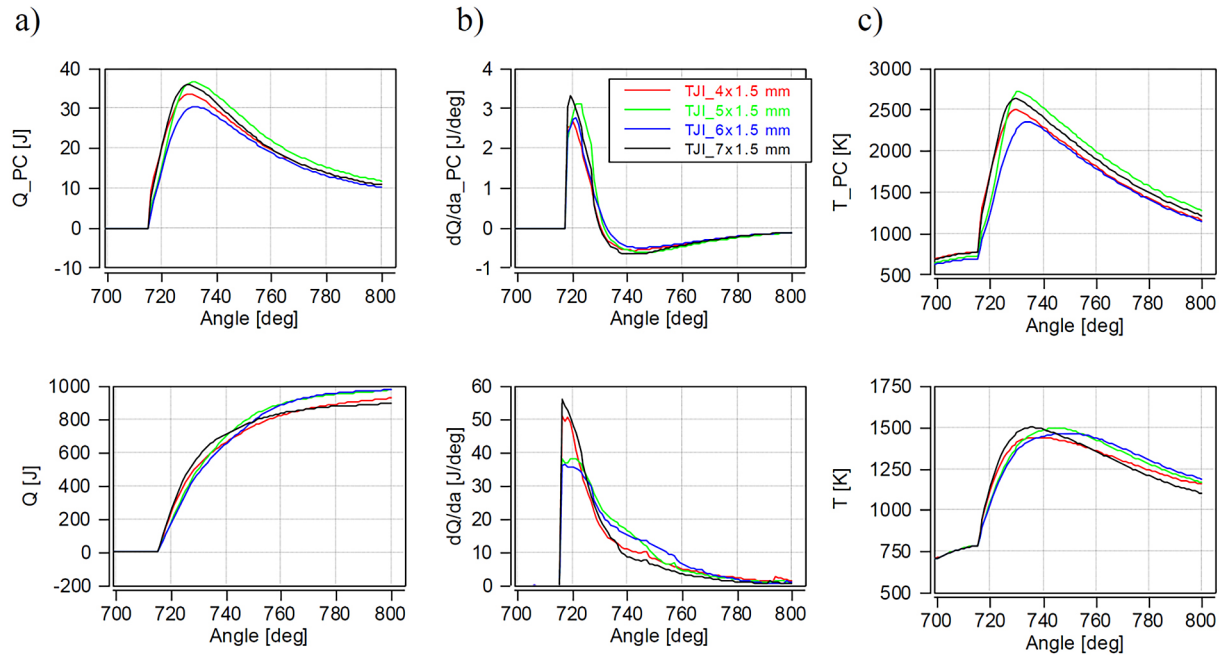


**Figure 7.** Profiles of thermodynamic indicators in a one-dimensional model (for the pre-chamber and the main combustion chamber): a) heat release, b) heat release rate, c) temperature in a TJI system with a variable number of pre-chamber orifices of constant diameter

from the PC holes to MC. Analysis of the data in Figure 8 indicates the highest rate for the system with four holes. The flames reach an outflow rate of over 300 m/s. With five holes, it is approximately 200 m/s, while the lowest velocity was recorded with  $n = 6$  holes. This may be due to the large excess air ratio during fuel ignition in the pre-chamber. Additionally, the maximum velocities with  $n = 4$  and 5 holes were achieved 1 deg earlier than with the remaining number of holes.

#### Assessment of nitric oxide (NO) concentration

Nitrogen oxide production is one of the key factors influencing the quality of the combustion process. The higher the NO fraction, the better the combustion quality due to the higher temperatures generated, which favours NO formation. Therefore, analysis of Figure 9 indicates that the NO concentration is highest in the PC with 4 holes. The difference between the remaining PC geometry cases is six-fold. Analysis of the entire combustion chamber indicates that these differences are not as significant, amounting to only about 25%. It should be noted that due to the initiation of the combustion process in PC and the significantly higher (almost twice as high – Figure 7) average temperature values, the NO share in PC is also almost 30 times higher.

Although the highest combustion pressures were obtained for the configuration with 7 orifices, other thermodynamic indicators (such as the amount of heat released in both chambers and the temperature levels) point to the configuration with 5 orifices – at a constant diameter – as the overall best solution.

## VARIATION OF ORIFICE DIAMETER

#### Evaluation of charge formation processes

The previous analysis focused on changing the number of holes. The differences observed during these changes due to the change in flow cross-section were quite significant. Currently, the change concerns the number of holes while maintaining a constant flow diameter. This means that as the number of holes increases, their diameter decreases, achieving a constant flow cross-sectional area. Therefore, significantly smaller differences are expected between the individual test variants.

Figure 10 shows the changes in the excess air coefficient for different variants of the number and diameter of holes. Despite the same flow cross-sectional area, spatial changes in  $\lambda$  are clearly visible. For all variants (except  $n = 5$  holes), the value of  $\lambda$  in PC is close to stoichiometric. A more

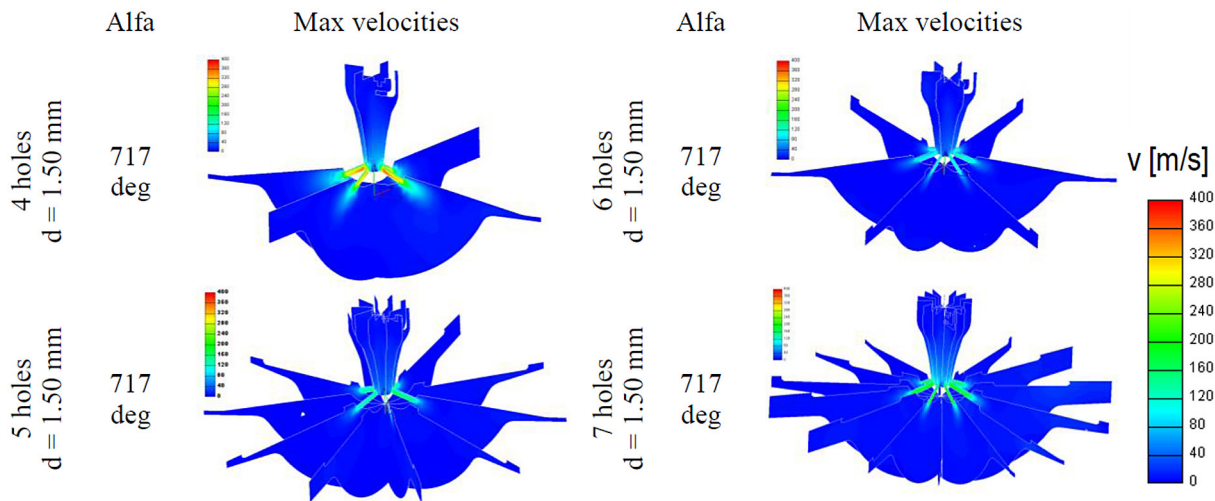


**Figure 8.** Flame jet discharge velocity from the pre-chamber in a TJI system with a variable number of constant-diameter orifices

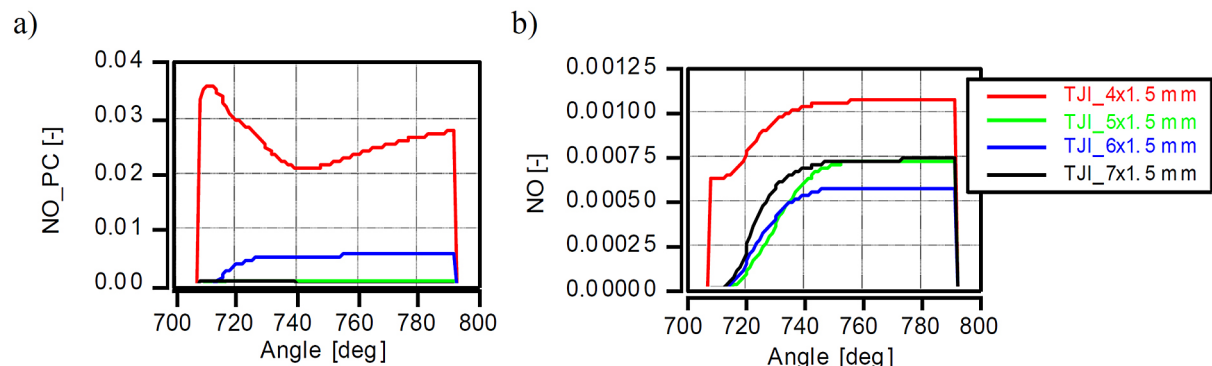


**Figure 9.** NO concentration profiles in the pre-chamber (a) and in the main combustion chamber (b) of a TJI system with a variable number of pre-chamber orifices of constant diameter

detailed analysis of each variant indicates that the location of the holes is significant, as the value of  $\lambda$  varies considerably in individual cross-sections. This is particularly evident in the 4-hole chamber.

Analysis of the global lambda-value in PC indicates that it is too low for each of the studied cases (Figure 11). The fuel dose to PC cannot be too high, as minimising it increases combustion efficiency. Experimental studies confirming this thesis were conducted by, among others, Pielecha et al. [20]. Due to the uniform flow diameter, a small number of holes increases TKE (turbulent kinetic energy). This results from the fact that the single flow window is the largest here, which supports the flow and increases the degree of charge swirl. In the case of global TKE values, there are practically no differences.

Due to the significant similarity of the  $\lambda$  distribution (local in PC and global) and the global TKE, the cylinder pressure curve is very similar

(Figure 12). Differences in  $P_{mx}$  are minimal, amounting to a maximum of 2.5%. The highest-pressure value was obtained with  $n = 6$  holes and equal to 66.9 bar. It should be noted that the change in the pressure curve after ignition is completely similar and convergent for all cases with the same flow diameter. This curve was completely different for a variable flow diameter (compare Figure 5).

#### Assessment of thermodynamic conditions

The thermodynamic analysis of the combustion process in the pre-chamber is very similar (Figure 13). Except for the 5-hole case, the other variants have a similar temperature distribution in PC, but only in the 4-hole case is the temperature development the fastest. This may indicate a high heat release rate in this chamber. As before, such a temperature distribution in the pre-chamber may

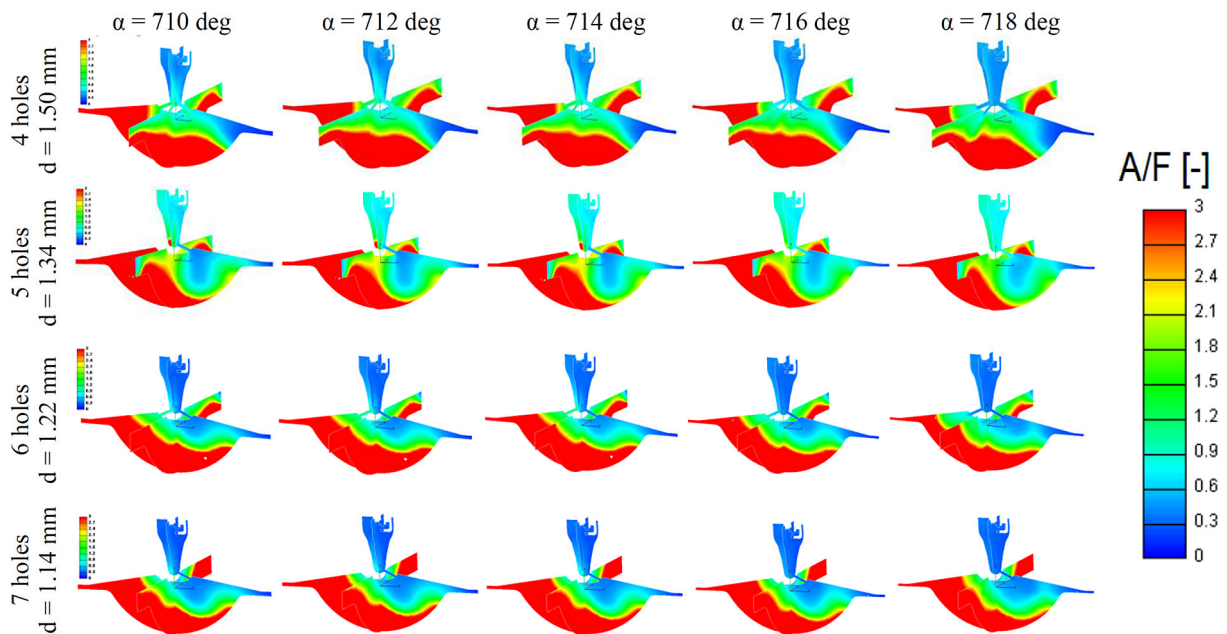


**Figure 10.** Distribution of the air-fuel equivalence ratio in a TJI system with a variable number and diameter of pre-chamber orifices (at a constant total flow area through the pre-chamber)

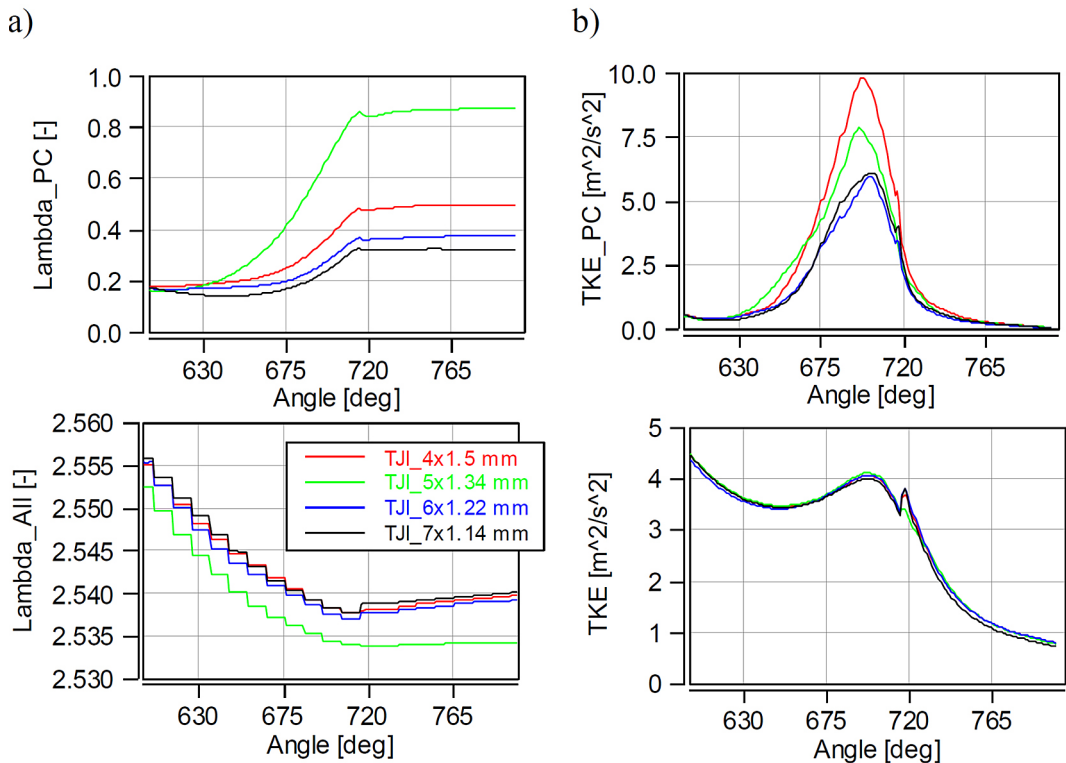
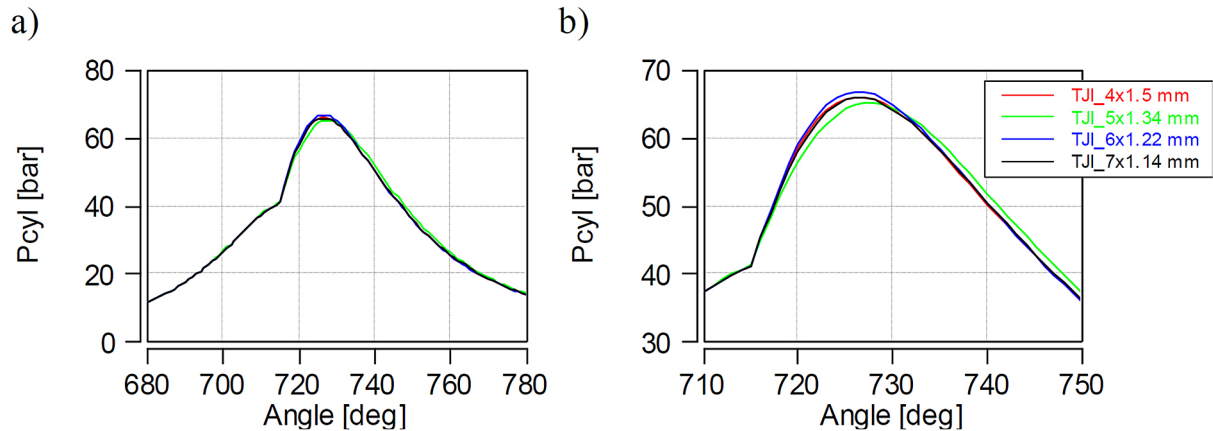


**Figure 11.** Variation of the mean lambda (a) and TKE (b) values in the pre-chamber and the main combustion chamber of a TJI system with a variable number and diameter of pre-chamber orifices (at a constant total flow area through the pre-chamber)

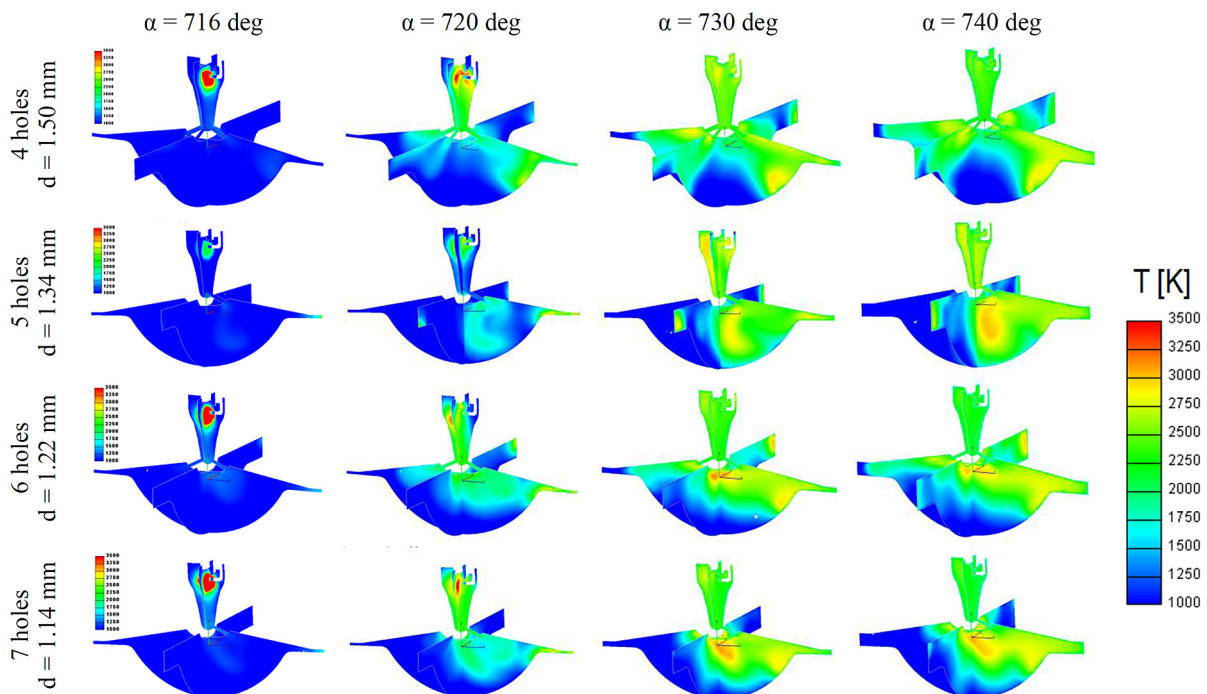
result from the ease of flow through the largest diameter of the holes from PC to MC.

Figure 14 shows that heat is released fastest in PC in the 4-hole chamber and reaches the highest

value first ( $Q_{mx\_PC} = 33.6$  J). The 5-hole case achieves a higher value, but slightly later ( $Q_{mx\_PC} = 35.7$  J). The scatter of  $Q_{mx\_PC}$  values is not large and amounts to 15%. The maximum



**Figure 12.** Variation of in-cylinder pressure (a) and its and an enlarged view of the selected scale segment (b) in a TJI system with a variable number and diameter of pre-chamber orifices (at a constant total flow area through the pre-chamber)



**Figure 13.** Temperature field distribution in a turbulent jet ignition (TJI) system with variable number and diameter of pre-chamber orifices at constant total flow area

value in the entire chamber is the largest at  $n = 4$  holes and amounts to 931 J. For the other combustion chamber geometries, the change in value oscillates within the range of only 6%.

The heat release rate in the PC is maximum at  $n = 4$  holes ( $dQ_{mx\_PC} = 2.66$  J/deg). These values are very similar within 15%. The total heat release rate is maximum at  $n = 6$  holes ( $dQ_{mx} = 54.9$  J/deg). The maximum value changes by approximately 18% (the largest changes at  $n = 5$  holes).

Analysis of the temperature values in PC shows – as in the case of  $dQ_{da\_PC}$  – a very

similar pattern: the highest values are achieved most quickly by the 4-hole system ( $T_{mx\_PC} = 2502$  K). However, the highest temperature values are also consistent with  $dQ_{da}$  for the 5-hole system ( $T_{mx\_PC} = 2645$  K).

The maximum temperature values in the main chamber are also highest for the 5-hole system ( $T_{mx} = 1493$  K). The changes in the maximum value are very small, amounting to only 4%. Compared to the case of a variable number of holes,  $T_{mx}$  values above 1500 K have not been achieved at present.

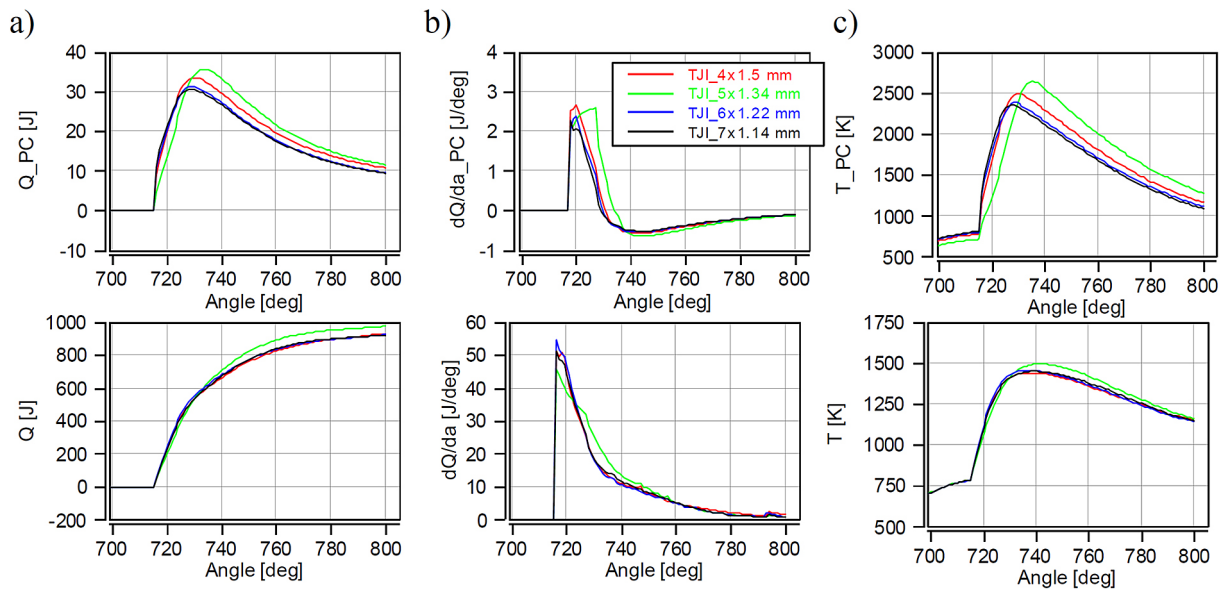


**Figure 14.** One-dimensional thermodynamic profiles – heat release (a), heat release rate (b), and temperature (c) in a TJI system with variable number and diameter of pre-chamber orifices at constant total flow area

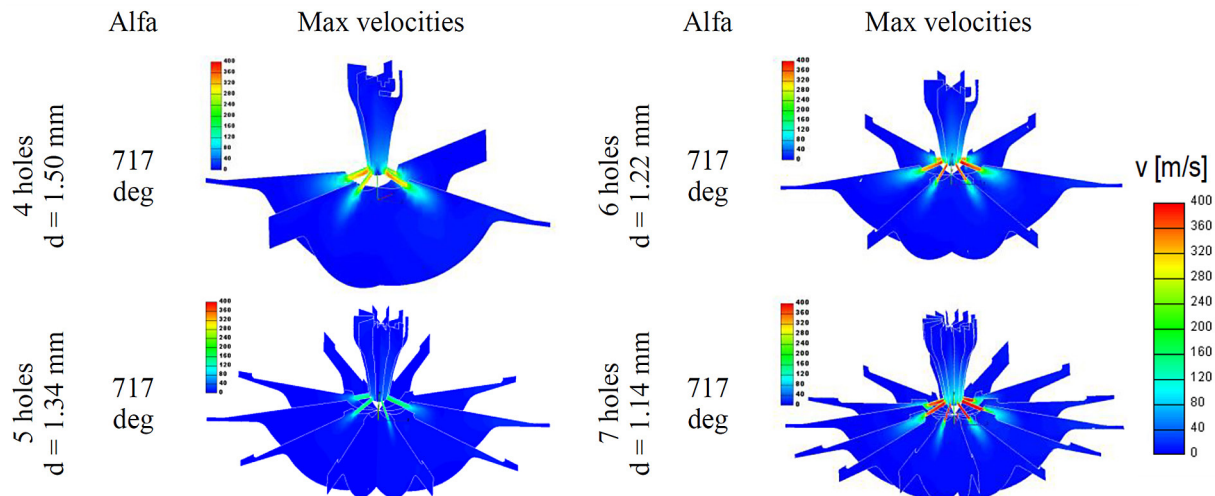


**Figure 15.** Flame jet discharge velocity from the pre-chamber in a TJI system with variable number and diameter of constant-flow-area orifices

#### Assessment of the mixture discharge velocity from the pre-chamber

Since the first 4-hole case is the same as before, it is known that the outflow velocity of the torch was approximately 300 m/s. Analysis of Figure 15 indicates that this is not the maximum value. Significantly higher values were obtained for  $n = 6$ . The highest values (360–400 m/s) were obtained for  $n = 7$ . This may be because the hole diameters are the smallest, and for the same flow area at similar combustion pressure values, the outflow velocity must be the highest.

#### Assessment of nitric oxide (NO) concentration

The nitrogen oxide concentration is at a similar level as in the case of constant hole diameter (Figure 9). However, in the pre-chamber and main chamber, no significant changes were noted compared to previous studies. In this research, (Figure 16), similar NO values were observed, differing from the previous ones by less than 10%. Again, the highest NO values result from the large flame flow area and combustion initiation in the main chamber.

The studies above do not clearly define the best TJI system variant for hydrogen combustion. Therefore, further work was undertaken to

determine the single most advantageous variant from the cases studied.

Most of the results from the analyses above indicate that the configuration with 5 orifices – at varying diameters – provides the best overall performance (maximum heat release and maximum temperature).

## INFLUENCE OF ORIFICE NUMBER AND DIAMETER VARIATION

The combustion efficiency was also determined as the amount of energy produced  $Q$  to the energy supplied with the fuel, defined by the equation:

$$\eta_{comb} = \frac{Q}{(qo_{MC} + qo_{PC}) \cdot LHV} \quad (1)$$

where:  $qo$  denotes the dose fed to the pre-chamber and main chamber, respectively, and

$LHV$  denotes the calorific value of hydrogen (120 MJ/kg).

Analysis of the data in Figure 17 indicates that the highest combustion efficiency was achieved for the 6-hole variant at  $d = 1.5$  mm. However, the smallest changes between the two variants were obtained with  $n = 5$  holes.

Therefore, a larger number of indicators should be considered to determine the most favourable combustion system variant (from those analysed). On the basis of the results above, the best variant of the pre-chamber was assessed. Multi-criteria evaluation was used, which assigned weights to the appropriate thermodynamic quantities according to Table 4.

All parameters were assigned equal weights (1/13), as no more important parameters were distinguished, which determine the charge preparation and combustion process. The excess air coefficient (lambda) and charge swirl (TKE) influence charge preparation and the

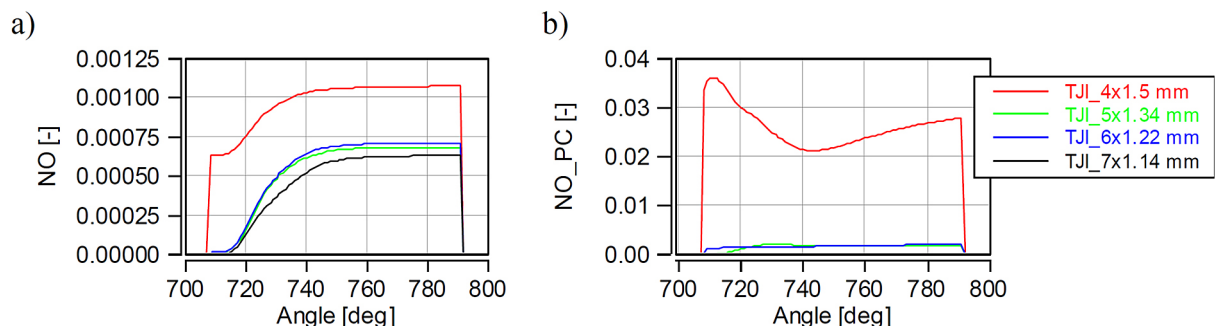


**Figure 16.** NO concentration in the pre-chamber (a) and main combustion chamber (b) of a TJI system with variable number and diameter of pre-chamber orifices at constant total flow area

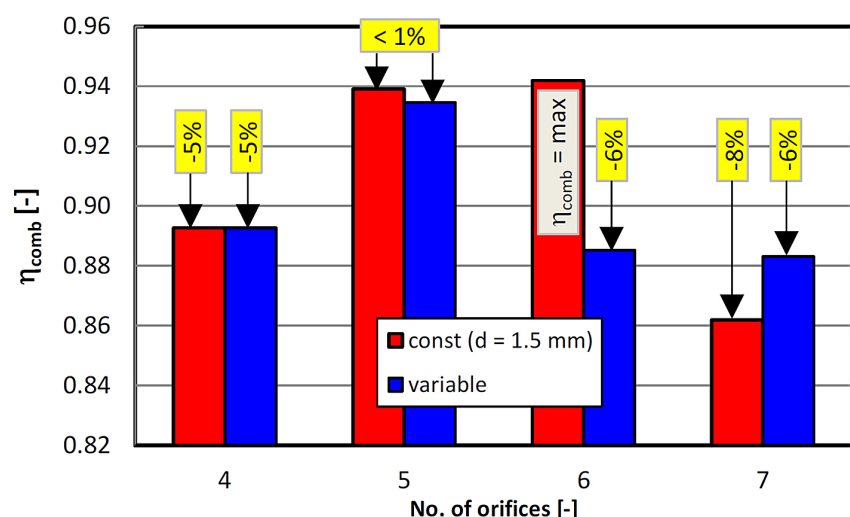


**Figure 17.** Analysis of combustion efficiency for the investigated combustion chamber configurations

homogenization of the fuel-air mixture. Therefore, three variants were determined to achieve the best combustion system:

- For a variable number of holes with a constant diameter (for PC and the entire combustion chamber)
- For a variable number of holes and diameters with a constant flow diameter (for PC and the entire combustion chamber)
- The third variant involves jointly determining the best solution, taking into account the number and fixed and variable diameter of the holes.

The maximum values of the indicators presented above were compared based on Table 5.

The amount of heat released was not analysed due to the combustion efficiency presented, which already considers the amount of heat released. Furthermore, due to the inability to measure only the combustion pressure in PC, this value was included only for the full combustion system. The target function based on these assumptions was created as:

$$f(U) = \sum_{i=1}^n m_i X_i \rightarrow \max \quad (2)$$

where:  $n$  – number of variables,  $m$  – variable's impact indicator (where  $\sum m_i = 1$ );  $i$  – the analysed variable.

**Table 4.** Determination of the weight contributions of individual variables in the combustion process study

| No. | Parameter   | Weight          | Objective (minimisation/maximisation) |
|-----|---|-----------------|---------------------------------------|
| 1.  | $P_{\max}$  | 1/13            | Max                                   |
| 2.  | $(dQ/d\alpha)_{\max\_PC}; (dQ/d\alpha)_{\max}$                              | $2 \times 1/13$ | Max                                   |
| 3.  | $T_{\max\_PC}; T_{\max}$  | $2 \times 1/13$ | Max                                   |
| 4.  | $\eta_{\max\_PC}; \eta_{\max}$  | $2 \times 1/13$ | Max                                   |
| 5.  | Lambda <sub>PC</sub> ; Lambda <sub>(<math>\alpha_{\text{ign}}</math>)</sub> | $2 \times 1/13$ | Near 1                                |
| 6.  | TKE <sub>PC</sub> ; TKE <sub>(<math>\alpha_{\text{ign}}</math>)</sub>       | $2 \times 1/13$ | Max                                   |
| 7.  | NO <sub>PC</sub> ; NO   | $2 \times 1/13$ | Max                                   |

**Table 5.** Analysis of normalised values for constant and variable orifice diameter cases

| Variable                 | u [-]  | const d = 1.5 mm |       |       |       | variable d |        |        |        |
|--------------------------|--------|------------------|-------|-------|-------|------------|--------|--------|--------|
|                          |        | 4×1.5            | 5×1.5 | 6×1.5 | 7×1.5 | 4×1.5      | 5×1.34 | 6×1.22 | 7×1.14 |
| Tmx <sub>PC</sub>        | 0.0769 | 0.030            | 0.077 | 0.000 | 0.059 | 0.039      | 0.077  | 0.008  | 0.000  |
| dQmx <sub>PC</sub>       | 0.0769 | 0.000            | 0.056 | 0.015 | 0.077 | 0.077      | 0.064  | 0.022  | 0.000  |
| NO <sub>PC</sub>         | 0.0769 | 0.077            | 0.001 | 0.016 | 0.000 | 0.077      | 0.000  | 0.006  | 0.000  |
| $\eta_{\text{comb\_PC}}$ | 0.0769 | 0.039            | 0.077 | 0.000 | 0.069 | 0.045      | 0.077  | 0.011  | 0.000  |
| TKE <sub>PC</sub>        | 0.0769 | 0.010            | 0.000 | 0.077 | 0.004 | 0.077      | 0.039  | 0.000  | 0.003  |
| $\lambda_{\text{PC}}$    | 0.0769 | 0.038            | 0.060 | 0.047 | 0.045 | 0.038      | 0.067  | 0.029  | 0.026  |
| Tmx                      | 0.0769 | 0.000            | 0.072 | 0.030 | 0.077 | 0.000      | 0.077  | 0.024  | 0.013  |
| dQmx                     | 0.0769 | 0.058            | 0.007 | 0.000 | 0.077 | 0.049      | 0.000  | 0.077  | 0.047  |
| NO                       | 0.0769 | 0.077            | 0.000 | 0.039 | 0.051 | 0.077      | 0.047  | 0.000  | 0.043  |
| $\eta_{\text{comb}}$     | 0.0769 | 0.030            | 0.074 | 0.077 | 0.000 | 0.014      | 0.077  | 0.008  | 0.000  |
| P                        | 0.0769 | 0.038            | 0.000 | 0.077 | 0.031 | 0.038      | 0.000  | 0.077  | 0.031  |
| TKE                      | 0.0769 | 0.000            | 0.002 | 0.077 | 0.008 | 0.039      | 0.077  | 0.077  | 0.000  |
| $\lambda$                | 0.0769 | 0.074            | 0.074 | 0.072 | 0.074 | 0.074      | 0.074  | 0.074  | 0.074  |
| Final                    |        | 0.471            | 0.501 | 0.526 | 0.572 | 0.642      | 0.675  | 0.412  | 0.236  |
| Const/variable diameter  |        | 4                | 3     | 2     | 1     | 2          | 1      | 3      | 4      |
| All chamber              |        | 6                | 5     | 4     | 3     | 2          | 1      | 7      | 8      |

The above equation was applied to 4 calculation variants (one series includes the pre-chamber and the full combustion system). The maximum values in Table 5 were normalised to 1. Weights were taken into account, and the results of this operation were presented in Table 5 in accordance with Equation 2. On the basis of Table 5, the following conclusions can be drawn:

- For a constant pre-chamber orifice diameter, the best solution is to increase the number of orifices. This increases the flow cross-section and thus reduces interchamber flow losses. Analysis of the data in Table 5 indicates that reducing the number of orifices reduces the objective function value by several percent (8% for 6 orifices, 12% for 5 orifices, and 18% for 4 orifices).
- For a constant flow diameter (variable orifice diameter), the best solution is the five-orifice variant with a diameter of 1.34 mm. This solution is slightly better than the chamber geometry with 4 orifices. Increasing the number of orifices to 6 reduces the final index by 30% (probably due to the reduction in the flow diameter of a single orifice). The use of a 7-hole chamber results in a reduction of the swirl in PC (the lowest TKE value), a deterioration of the combustion efficiency and a reduction of the objective function value by more than 70%.

Considering all investigated variants (with different numbers of orifices and either constant or variable diameter), the configuration with 5 orifices of 1.34 mm diameter also proves to be the best solution.

## CONCLUSIONS

On the basis of the simulation work conducted regarding the number and diameter of PC holes, the following general conclusions were drawn:

1. The effect of the number of holes in the PC (Variant I) is much greater than the effect of diameter (Variant II) on the thermodynamic and emission parameters of the combustion engine. Much greater changes in the first variant result from the variable flow cross-section, which affects interchamber flow conditions and the variability of thermodynamic processes.
2. Changes in thermodynamic parameters begin with charge preparation through interchamber flows and final combustion in the main chamber, regardless of the test variant.

The detailed conclusions from the above studies are as follows:

- 1) While maintaining a constant pre-chamber hole diameter ( $d = 1.5$  mm), increasing their number improves the combustion process by increasing the total flow cross-section, thereby reducing flow losses between the pre-chamber and the main chamber. Reducing the number of holes results in a deterioration of engine performance compared to the best-performing case. This means that a larger number of holes reduces flow losses and thus promotes ignition stabilisation.
- 2) While maintaining a constant cross-sectional area, the diameter of individual holes is most important. The best results were obtained for a pre-chamber with 5 holes of approximately 1.34 mm in diameter. This case achieved the best results compared to the others in this variant. Increasing the number of holes (reducing their diameter accordingly) led to a significant deterioration of operating conditions compared to the best case. This confirms that the number of holes has the greatest impact on the combustion process dynamics, while the diameter of a single hole should be selected so that its size prevents flame extinction (the critical diameter is approximately 0.29 mm). The best configuration for the analysed variants is a pre-chamber with 5 holes of approximately 1.34 mm in diameter.

## REFERENCES

1. Fan B., Wu X., Pan J., Qi X., Fang J., Lu Q., Zhang Y. Research on the structure of pre-chamber and jet orifice of a turbulent jet ignition rotary engine fueled with methanol/gasoline blends. *Appl. Therm. Eng.* 2023; 229: 120588. <https://doi.org/10.1016/j.applthermaleng.2023.120588>
2. Lu Y., Qian Y., Zhang D., Chen Y., Pei Y. Parameters optimization of prechamber jet disturbance combustion system – effect of prechamber volume and fuel injection mass ratios on performance and exhausts in a diesel engine. *Fuel* 2024; 373: 132360. <https://doi.org/10.1016/j.fuel.2024.132360>
3. Cui Z., Tian J., Zhang X., Yin S., Long W., Song H. Experimental study of the effects of pre-chamber geometry on the combustion characteristics of an ammonia/air pre-mixture ignited by a jet flame. *Processes* 2022; 10(10): 2102. <https://doi.org/10.3390/pr10102102>
4. Zhao D., An Y., Pei Y., Hu J., Wang C., Sun Y., Xu L., Zhang Z., Sun J. Numerical study on the

inner spray and combustion of active pre-chamber jet ignition for achieving higher performance of a hybrid engine under ultra-lean conditions. *Energy* 2024; 309: 133149. <https://doi.org/10.1016/j.energy.2024.133149>

5. Jeelan Basha K.B., Balasubramani S., Sivasankaralingam V. Effect of pre-chamber geometrical parameters and operating conditions on the combustion characteristics of the hydrogen-air mixtures in a pre-chamber spark ignition system. *Int. J. Hydrog. Energy* 2023; 48(65): 25593–608. <https://doi.org/10.1016/j.ijhydene.2023.03.308>
6. Zhou L., Song Y., Hua J., Liu F., Liu Z., Wei H. Effects of different hole structures of pre-chamber with turbulent jet ignition on the flame propagation and lean combustion performance of a single-cylinder engine. *Fuel* 2022; 308: 121902. <https://doi.org/10.1016/j.fuel.2021.121902>
7. Chen R., Li T., Wei Q., Guo X., Wu Z., Huang S., Li S., Wei W. Prechamber pressure and heat release characteristics controlled by active prechamber structure parameterization. *SSRN*; 2025. <https://doi.org/10.2139/ssrn.5106394>
8. Hua J., Zhou L., Gao Q., Feng Z., Wei H. Influence of pre-chamber structure and injection parameters on engine performance and combustion characteristics in a turbulent jet ignition (TJI) engine. *Fuel* 2021; 283: 119236. <https://doi.org/10.1016/j.fuel.2020.119236>
9. Trombley G. and Toulson E. A fuel-focused review of pre-chamber initiated combustion. *Energy Convers. Manag.* 2023; 298: 117765. <https://doi.org/10.1016/j.enconman.2023.117765>
10. Zhao W., Pan J., Wei H., Chen L. Synergy effect of nozzle structure and pre-chamber reactivity on the combustion characteristics of ammonia engines. *Fuel* 2025; 381: 133360. <https://doi.org/10.1016/j.fuel.2024.133360>
11. Liu P., Zhong L., Zhou L., Wei H. The ignition characteristics of the pre-chamber turbulent jet ignition of the hydrogen and methane based on different orifices. *Int. J. Hydrog. Energy* 2021; 46(74): 37083–97. <https://doi.org/10.1016/j.ijhydene.2021.08.201>
12. Onofrio G., Napolitano P., Tunestål P., Beatrice C. Combustion sensitivity to the nozzle hole size in an active pre-chamber ultra-lean heavy-duty natural gas engine. *Energy* 2021; 235: 121298. <https://doi.org/10.1016/j.energy.2021.121298>
13. Yang J., Xie F., Jiang B., Li X., Su Y., Zhang H. Influence of structure parameters of pre-chamber on lean combustion of active pre-chamber jet ignition engine. *Energy* 2024; 304: 132053. <https://doi.org/10.1016/j.energy.2024.132053>
14. Wei F., Wang Q., Cao J., Cui Z., Long W., Tian H., Tian J., Dong D., Wang Y. Experimental study of the ignition chamber with accelerating cavity applying to methanol lean combustion. *Fuel* 2024; 355: 129358. <https://doi.org/10.1016/j.fuel.2023.129358>
15. Hlaing P., Echeverri Marquez M., Cenker E., Im H.G., Johansson B., Turner J.W.G. Effects of volume and nozzle area in narrow-throat spark-ignited pre-chamber combustion engines. *Fuel* 2022; 313: 123029. <https://doi.org/10.1016/j.fuel.2021.123029>
16. Biswas S., Tanvir S., Wang H., Qiao L. On ignition mechanisms of premixed CH<sub>4</sub>/air and H<sub>2</sub>/air using a hot turbulent jet generated by pre-chamber combustion. *Appl. Therm. Eng.* 2016; 106: 925–37. <https://doi.org/10.1016/j.applthermaleng.2016.06.070>
17. Qin F., Shah A., Huang Z., Peng L., Tunestal P., Bai X.-S. Detailed numerical simulation of transient mixing and combustion of premixed methane/air mixtures in a pre-chamber/main-chamber system relevant to internal combustion engines. *Combust. Flame* 2018; 188: 357–66. <https://doi.org/10.1016/j.combustflame.2017.10.006>
18. Wakasugi T., Tsuru D., Watanabe H. Multijet pre-chamber ignition using hydrogen and methane: effects of fuel composition and orifice diameter on ammonia combustion in a large-bore chamber. *Fuel* 2026; 405: 136499. <https://doi.org/10.1016/j.fuel.2025.136499>
19. Frasci E., Novella Rosa R., Plá Moreno B., Arsie I., Jannelli E. Impact of prechamber design and air–fuel ratio on combustion and fuel consumption in a SI engine equipped with a passive TJI. *Fuel* 2023; 345: 128265. <https://doi.org/10.1016/j.fuel.2023.128265>
20. Soltic P., Hilfiker T., Hänggi S. Efficient light-duty engine using turbulent jet ignition of lean methane mixtures. *Int. J. Engine Res.* 2021; 22(4): 1301–11. <https://doi.org/10.1177/1468087419889833>
21. Balmelli M., Rogers D., Hilfiker T., Wright Y., Soltic P. Method for pressure trace based thermodynamic analysis of pre-chamber combustion. *Energy Convers. Manag.* 2024; 312: 118561. <https://doi.org/10.1016/j.enconman.2024.118561>
22. Aoyagi T., Wakasugi T., Tsuru D., Tashima H. Effects of torch flame strength on the combustion process in medium-speed gas engines through pre-chamber orifice specifications. *Combustion Engines*. 2025; 202(3): 44–57. <https://doi.org/10.19206/CE-205609>
23. Wei W., Chen R., Li T., Wei Q., Guo X., Wu Z., Huang S., Li S. Prechamber pressure and heat release characteristics controlled by active pre-chamber structure parameterization. *Appl. Therm. Eng.* 2025; 278: 127190. <https://doi.org/10.1016/j.applthermaleng.2025.127190>
24. Hu J., Pei Y., An Y., Zhao D., Zhang Z., Sun J., Gao D. Study of active pre-chamber jet flames based on the synergy of airflow with different nozzle swirl angle. *Energy*. 2023; 282: 128198. <https://doi.org/10.1016/j.energy.2023.128198>

25. Sharma P., Marquez M.E., Luo X., Cenker E., Turner J.W.G., Magnotti G. Flame development in prechamber assisted engine: high-speed PLIF. *Proc. Combust. Inst.* 2024; 40(1–4): 105245. <https://doi.org/10.1016/j.proci.2024.105245>

26. Alvarez C.E.C., Couto G.E., Roso V.R., Thiriet A.B., Valle R.M. A review of prechamber ignition systems as lean combustion technology for SI engines. *Appl. Therm. Eng.* 2018; 128: 107–20. <https://doi.org/10.1016/j.applthermaleng.2017.08.118>

27. Turkyilmazoglu M. Laminar slip wall jet of Glauert type and heat transfer. *Int. J. Heat Mass. Transf.* 2019; 134: 1153–8. <https://doi.org/10.1016/j.ijheatmasstransfer.2019.02.051>

28. Turkyilmazoglu M. Combustion of a solid fuel material at motion. *Energy*. 2020; 203: 117837. <https://doi.org/10.1016/j.energy.2020.117837>

29. Chi C. and Thévenin D. DNS study on reactivity stratification with prechamber H<sub>2</sub>/air turbulent jet flame to enhance NH<sub>3</sub>/air combustion in gas engines. *Fuel*. 2023; 347: 128387. <https://doi.org/10.1016/j.fuel.2023.128387>

30. Yin Y., Wang S., Wang Z. A LES study on the instantaneous H<sub>2</sub> jet-ignited combustion characteristics of H<sub>2</sub>/NH<sub>3</sub> mixtures. *Int. J. Hydrog. Energy*. 2024; 86: 382–94. <https://doi.org/10.1016/j.ijhydene.2024.08.429>

31. Wang P., Long W., Pang B., Xu X., Liu S., Wang J., Zhang X., Dong P., Wang Y. Investigation on ignition chamber performance in a methanol-fueled TJI-HPDI engine: Synergy of nozzle structure, swirl ratio, and spray angle. *Energy*. 2025; 330: 136957. <https://doi.org/10.1016/j.energy.2025.136957>

32. Pielecha I., Bueschke W., Skowron M., Fiedkiewicz Ł., Szwajca F., Cieślik W., Wislocki K. Prechamber optimal selection for a two stage turbulent jet ignition type combustion system in CNG-fuelled engine. *Combustion Engines*. 2019; 176(1): 16–26. <https://doi.org/10.19206/CE-2019-103>